Remote Sensing with Reflected Signals

GNSS–R Data Processing Software and Test Analysis

DONGKAI YANG, YANAN ZHOU, AND YAN WANG

(airplane) © istockphoto.com/Mark Evans; gpsiff background

Authors from a leading Chinese university describe how reflected GNSS signals can be used in sea-wind retrieval, seawater salinity detection, ice-layer density measurement and other remote sensing applications. They introduce the GNSS-R concept, demonstrate the characteristics of the GPS reflected signal, and describe their data-processing method for exploiting the reflected signals. The article includes test results from field trials gathering data over maritime and grassland areas.

Generally, a multipath signal in positioning is often considered an undesirable phenomenon that needs to be suppressed. A reflected GNSS signal is one kind of multipath, also known as a *scattered* signal. Usually, the reflected signal is regarded as an error source that deteriorates the positioning accuracy. But, in fact, these scattered signals can be used in many remote sensing applications.

This article will introduce the GNSS-reflection (GNSS-R) remote sensing concept and, taking GPS reflected signals as an example, demonstrate the characteristics of the these signals and our method for processing them to extract environmental data of interest. Then, we will describe our software-based receiving and processing system and tests performed for data collection over sea and grassland areas, presenting the related results.

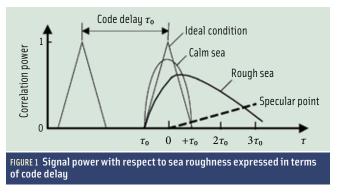## GNSS–R Remote Sensing: The Concept

GNSS-reflection (GNSS-R) remote sensing is a new category of satellite navigation applications. Essentially, it entails a method of remote sensing that receives and processes microwave signals reflected from various surfaces to extract useful information about those surfaces.

In this process, the GNSS L-band satellite acts as the transmitter and an airplane or low earth orbit (LEO) satellite, as the receiving platforms. For altimetry applications, a GNSS-R receiver can also be placed on the land.

The advantages of GNSS-R remote sensing over satellite scatterometry and radar altimetry are as follows:
1) no additional transmitter;
2) plenty of signal sources, including GPS, Galileo, GLONASS, and Beidou/Compass;
3) use of spread-spectrum communication technology to enable the receiver to receive weak signals;
4) wide range of uses for such things as sea-wind retrieval, seawater salinity

40 InsideGNSS   SEPTEMBER/OCTOBER 2009   www.insidegnss.com

FIGURE 1 **Signal power with respect to sea roughness expressed in terms of code delay**

FIGURE 2 **Reflection area**

FIGURE 3 **Comparison between direct and reflected signal**

detection, ice-layer density measurement, humidity measurement of land, and detection of moving targets.

Take sea-wind retrieval, for example: the reflected signals provide a rough correlation with independent measurements of the sea wind.

Figure 1 shows the signal power of scattered signal with respect to sea roughness.

Figure 2 further defines the subsections of a signal reflection region and the associated effects on a GNSS signal. The blue arrow indicates the *specular point*, where the reflected signal is the strongest. The red ellipses represent the *equal-code delay* lines, and we call the uneven ring belts between them *Fresnel zones*. The black curves are the *equal-Doppler lines*. Finally, the small black region is a *resolution cell* formed by the crossing of Fresnel zones and Doppler lines.

For the GPS reflected signal, the strong reflection at L-band frequencies from water and metal surfaces can help reception of weak signals. GPS satellites are far from the Earth and the Fresnel belts are small, about 0.01 and 0.4 kilometers as observed from airplane and satellite platforms, respectively. Through analyzing the reflected signal and comparing it with the direct one, we can extract some characteristic parameters about the reflection surface.

Characteristics of GPS Reflected Signal

Reflected GPS signals have a distinct *signature* or set of characteristics that are different from directly received signals. Some of the most important are:

1) Polarization. The GPS signal is right-hand circular polarized. When it is reflected by the surface, the signal might change into left-hand polarization. So, a left-hand circular polarization (LHCP) antenna is used to collect reflected data.

2) Code delay and Doppler shift. The reflected signal has to propagate an extra path segment compared with the direct one, thus causing an additional time delay. In this article, we use the equation $2h \cdot \sin\theta = c\tau$ to estimate the extra delay of the specular point.

In a former study, we considered the Dopplers of the direct and reflected signals as being the same, but, in fact, the Doppler changes after reflection. Taking this into account, first we use the Doppler of direct signal as that of the reflected one, and after calculation, we can get the true Doppler of the reflected signal.
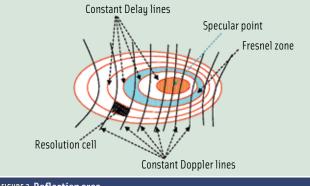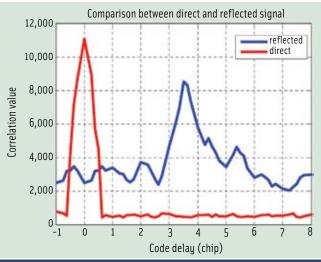
3) Correlation. The correlation characteristic can be expressed by the integral function of correlation. For the direct signal, it can be described as:

$$Y(t) = \int_0^{T_i} a(t) \cdot s(t)dt \qquad (1)$$

But for the reflected signal, it is:

$$Y(\tau, \tau_0, t) = \int_0^{T_i} a(t + \tau_0 - \tau) \cdot s(t + \tau_0)dt \qquad (2)$$

where

$a(t)$: local C/A code sequence
$s(t)$: data received by the receiver
T_i : time interval of integration
τ_0: estimated code delay of specular point
τ : code delay within $\{-M, +N\}$ which need to be determined by the user.

We get significant correlation only if the code delay of $a(t)$ and $s(t)$ is the same and the Doppler shift between them is correctly compensated.

Figure 3 compares the direct and reflected signals in terms of code delay. The data was collected in a flight trial at an altitude of about 600 meters. The results show that, compared with the direct signal, the reflected signal's peak value arrives about 3.5 chips later, and the peak correlation value is lower.
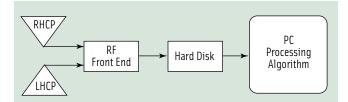
FIGURE 4 **Comparison between direct and reflected signal**

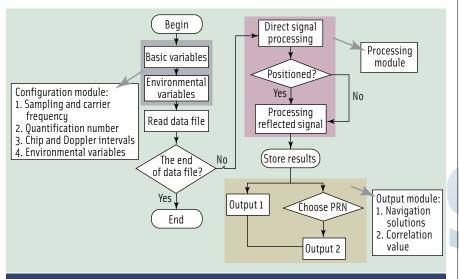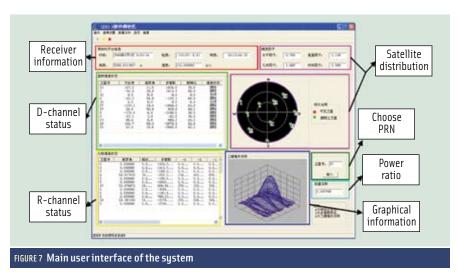FIGURE 5 **Antennas: LHCP antenna (left) and RHCP antenna (right)**

FIGURE 6 **Software flowchart**

FIGURE 7 **Main user interface of the system**

System Architecture

The GNSS-R processing system consists of a software-based GPS receiver with a pair of antennas (one right-hand polarized and the other left-hand polarized for reception at the L1 band) and dual front-ends, and a PC for signal processing. The front-end is used to down-convert the GPS signal to 4.6420 MHz and digitize it with two bits at a sampling frequency of 20.454 MHz.

Figure 4 is a schematic of the hardware architecture. **Figure 5** shows the RHCP antenna, a general GPS aviation antenna for direct signal, and the LHCP antenna for reflected signal, a four-array antenna with a gain of 12 decibels. The PC contains the analyzing algorithm, serves as the processing platform, and outputs the results.
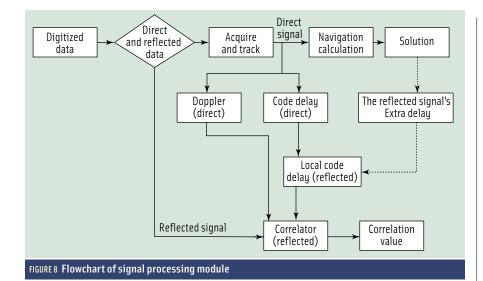
Software and Algorithm Details

The GNSS-R software has the overall tasks of reading the collected data, processing it, and outputting the solutions. At the same time, it must also provide the users with status information about each channel and facilitate user control.

The software has three main tasks: parameter configuration, signal processing, and outputting results both in data files and on a graphic display. (See **Figure 6**.)

Figure 7 shows the main user interface (UI) and highlights its seven key parts. On the left side of the UI screen, from top to bottom, are receiver information (including the position of the receiver, and such data as latitude, longitude, height, and speed), the status of 12 direct (D) channels, and the status of 12 reflected (R) channels.

The right side of the screen, from top to bottom, includes the distribution of satellites being tracked, the user-selectable PRN of the reflected channel, power ratio (that is, the power of direct signal over that of reflected signal), and the graphical information of the signal power with respect to code delay and Doppler, which changes as the data are calculated by the processing module.

The processing module, outlined in red in Figure 6, is the core module of the software system. Through comparing the direct signal with the reflected one, we can see that both the code delay and Doppler of the signal change after reflection. So, instead of seeking the maximum correlation peak, we compute the correlation power at different chips

FIGURE 8 Flowchart of signal processing module

FIGURE 9 Test system for dynamic sea reflected data collection

and frequencies away from the position of the prompt correlator, a technique that we call *open-loop processing*.

Figure 8 shows the processing flowchart of the signal-processing module. Once the direct channel has tracked one satellite, the reflected channel uses the direct channel's code delay and Doppler as reference. Then the reflected correlator calculates the correlating power at various chip and frequency intervals, according to the user's definition.

The dashed line refers to another processing approach. The extra delay caused by the additional path that the reflected signal has to travel could be calculated after determining the navigation solution, thus helping us find the true specular point that is the reflected

signal's peak value point with efficient processing.

Finally, through analyzing the power profile and subsequent modeling, we can extract the characteristic parameters of the reflecting surface. This latter step is not the focus of this paper; however, readers can find further information on this subject in the paper by V. U. Zavorotny et alia listed in the Additional Resources section at the end of this article.

Dynamic Test: Airborne Test Results

Figure 9 shows the test setup in an airplane that was used to collect sea-reflected data. The RHCP and LHCP antennas were mounted on the top and belly of
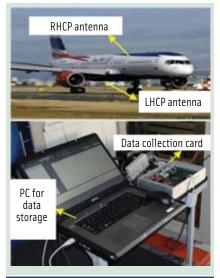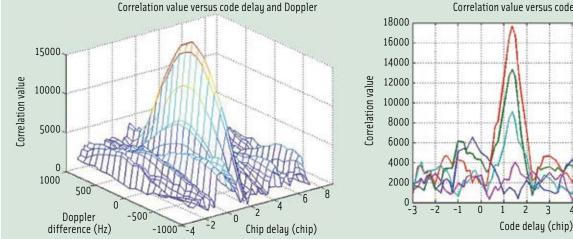
the plane, respectively, with the RHCP antenna zenith-oriented and the LHCP antenna nadir-oriented to collect signals reflected from the sea. The flying altitude was up to 5,000 meters with a maximum flying speed of 100 m/s.

The data on the left side of **Figure 10** represent results from the flight test in terms of the correlation value versus various code delay and Doppler values. The code and Doppler intervals are one-eighth chip and 100 Hertz, respectively.

The right-hand image shows that when the Doppler difference is 0 Hertz, the signal power is the strongest and gets weaker as the Doppler differences become bigger.

FIGURE 10 Test results: left, the correlation value versus code delay and Doppler differences; right, correlation value versus code delay at different Doppler differences
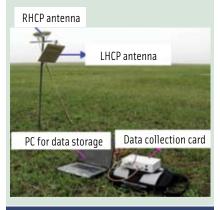
FIGURE 11 **Grassland test setup for reflected data collection**

FIGURE 12 **Reflection coefficient**

Static Test Results: Grassland

We use grassland static test data to demonstrate the possibility of using our system in remote sensing of land areas. **Figure 11** shows the test setup that was used to collect grassland reflected data.

Similar to the flight test, the RHCP and LHCP antennas were mounted on a shelf with the RHCP antenna oriented toward zenith and the LHCP antenna facing the grassland from which the signal reflections would arrive. After collecting data for a while, we poured water on the grassland to see if the reflected signal is sensitive to soil humidity.

Figure 12 shows the waveforms of the reflection coefficient (vertical scale). At point 211, we began to pour water on the reflecting surface, and we can see that the reflection coefficient becomes bigger after that.

Conclusions

This article introduced concepts about using GNSS-R in remote sensing and the related experiments we performed over sea and land using reflected GPS signals. We described our software-based receiving and processing system and displayed the processing results of the data collected in the two tests.

The results indicate that the reflected signal power is sensitive to the sea-wind and soil humidity, thus proving that our algorithm is correct and raising the possibility of using our software-based system in remote sensing.

Future work will include testing our system in other applications such as detecting the age of ice as well as improving the system accuracy for new applications.

Acknowledgment

Manufacturers

The GNSS-R processing system uses dual front-ends (RNSS-L1L1) from **Shijiazhuang New Century Electricity Technology Co., Ltd.**, Shijiazhuang, Hebei, China; RHCP antenna (S67-1575-39) from **Sensor Systems Inc.**, Chatsworth, USA; and LHCP antenna from **Beijing Dafang Technology Co.,Ltd.**, Beijing, China, and the data collecting card was developed by the **School of Electronic and Information Engineering Beihang University,** Beijing, China.

Additional Resources

[1] Belmonte Rivas, M., and M. Martin–Neira, "Coherent GPS reflections from the Sea Surface," *IEEE Geoscience and Remote Sensing Letters,* Vol. 3, No. 1, pp. 28–31, January 2006

According to the modeling and analyzing, we can obtain a measurement precision of 2 m/s for wind speed when the code interval is a half-chip and the Doppler interval is 250 Hertz.

[2] Esterhuizen, S., and D. Masters, D. Akos, and E. Vinande, "Experimental Characterization of Land-Reflected GPS Signals," *Proceedings of the ION GNSS 18th International Technical Meeting of the Satellite Division,* 2005

[3] Garrison J. L., and S. J. Katzberg and C. T. Howell," Detection of Ocean Reflected GPS Signals : Theory and Experiment," in *Proceedings of the IEEE Southeastern '97: Engineering the New Century[C],* Blacksburg, Virginia, pp. 290-294, 1997

[4] Garrison, J. L., and A. Komjathy, V. U. Zavorotny, and S. J. Katzberg, "Wind speed measurement using forward scattered GPS signals," *IEEE Transactions on Geosciences and Remote Sensing,* Vol. 40, No. 1, pp. 50–65, January 2002

[5] Gleason, S., and S. Hodgart, Y. P. Sun, C. Gommenginger, S. Mackin, M. Adjrad, and M. Unwin, "Detection and Processing of Bistatically Reflected GPS Signals from Low Earth Orbit for the Purpose of Ocean Remote Sensing," *IEEE Transactions on Geosciences and Remote Sensing,* Vol. 43, No. 6, pp. 1229–1241, June 2005

[6] Grant, M. S., and S. T. Acton and S. J. Katzberg, "Terrain Moisture Classification Using GPS Surface-Reflected Signals," *IEEE Geoscience and Remote Sensing Letters,* Vol. 4, No. 1, pp. 41–45, January 2007

[7] Lowe, S. T., and P. Kroger, G. Franklin, J. L. LaBrecque, J. Lerma, M. Lough, M.R. Marcin, R. J. Muellerschoen, D. Spitzmesser, and L. E. Young, "A Delay/Doppler-Mapping Receiver System for GPS-Reflection Remote Sensing," *IEEE Transactions on Geosciences and Remote Sensing,* Vol. 40, No. 5, pp. 1150–1163, May 2002

[8] Yang, D. K., and Y. Q. Zhang, Y. Lu, and Q. S. Zhang, "GPS Reflections for Sea Surface Wind Speed Measurement," *IEEE Geoscience and Remote Sensing Letters,* Vol. 5, No. 4, pp. 569–572, October 2008

[9] Zavorotny, V. U., and A. G. Voronovich and S. J. Katzberg, "Extraction of Sea State and Wind Speed from Reflected GPS signals: Modeling and Aircraft Measurements," in *Proceedings IGARSS 2000,* vol. 4, pp. 1507–1509, July 2000

Authors

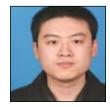**Dongkai Yang** is an associate professor in the School of Electronic and Information Engineering at Beihang University. He received his Ph.D. in communication and information systems from the Beihang University. His main research field is GNSS and related applications.

Yanan Zhou is a master's candidate in the School of Electronic and Information Engineering at Beihang University. She received her bachelor degree in communication engineeringfrom Hebei University of Technology. Her current research interests include the algorithm research and software development for GNSS-R software receiver.

Yan Wang is a master's candidate in the School of Electronic and Information Engineering at Beihang University. He received his bachelor's degree in communication engineering from Beijing University of Chemistry Technology. He is engaged in the algorithm research and correlator design for GNSS-R receivers. **IG**